Compact Cold-Atom Platform Based on Optical Grating and Planar Coil Chips

Chang-Jiang Huang[1,2†], Lei Xu[1,2†], Liang Chen[1,2], Chuan-Feng Li[1,2,3], Guang-Can Guo[1,2,3], Chang-Ling Zou[1,2,3*], and Guo-Yong Xiang[1,2,3*]

[1]*Laboratory of Quantum Information, University of Science and Technology of China, Hefei 230026, China*
[2]*CAS Center for Excellence in Quantum Information and Quantum Physics, University of Science and Technology of China, Hefei 230026, China*
[3]*Hefei National Laboratory, University of Science and Technology of China, Hefei 230088, China*

(Received 24 March 2025; accepted manuscript online 6 May 2025)

We present a compact cold atom platform where an optical grating chip and planar coil chip are placed inside a compact vacuum chamber to create a magneto-optical trap. This approach significantly reduces the system volume to about $20 \times 20 \times 20\,\mathrm{cm}^3$ compared to conventional vacuum systems and offers greater flexibility in accessing the trapped atoms. We demonstrate the trapping of 3×10^5 cold rubidium atoms at a temperature of $100\,\mu\mathrm{K}$ in a vacuum pressure below $10^{-7}\,\mathrm{mbar}$. The simplified optical geometry, low power consumption, and high degree of integration make this a promising platform for portable and versatile cold-atom devices in quantum sensing, timing, and information processing.

DOI: 10.1088/0256-307X/42/6/063102 CSTR: 32039.14.0256-307X.42.6.063102

1. Introduction. Cold atoms have become an essential tool for a wide range of applications, including matter-wave interferometers and optical clocks, for high-precision measurements.[1–5] They have also become increasingly important as a promising platform for quantum simulation and quantum computation.[6–14] These applications rely on the capability to cool and trap atoms using magneto-optical traps (MOTs),[15] which typically require bulky and complex apparatus for optical beams and magnetic coils. In particular, the strict alignment of six optical laser beams with the center of a quadratic magnetic field inside a vacuum chamber is experimentally challenging. In recent years, there has been growing interest in miniaturizing and simplifying MOT systems[16–33] to improve their portability, scalability, and ease of alignment. One major breakthrough was the development of grating MOTs,[16,17,21,22] which employ a single chip with diffraction gratings to generate the necessary laser cooling beams from a single input beam, significantly reducing the size and complexity of the optical setup. More recently, researchers have further streamlined MOT systems by replacing conventional anti-Helmholtz coils with planar coil chips, known as planar-integrated MOTs.[29,30] Efforts have also been made to miniaturize the traditionally cumbersome high-vacuum systems by utilizing customized vacuum chambers and passive vacuum pumps.[26,27,30]

Current planar-integrated MOTs are typically constructed by placing optical and magnetic field chips outside a glass vacuum cell.[17,29] However, this configuration has limitations. The working point of the planar-integrated MOT is confined to a limited height above the chip surface, and the presence of the glass cell wall gives rise to a small distance between the atom cloud and the wall, which imposes difficulties in optical access to the atom cloud and prevents the insertion of other functional photonic chip devices near the trapped atoms. Consequently, the integration of additional optical and electronic devices onto planar-integrated MOTs is hindered, such as transporting atoms trapped by the MOT to micrometers or even sub-micrometer distances from the chip surface.[34–46] Furthermore, glass cells are fragile, and the glass-to-metal flange limits the length of the cell. To fully realize the potential of integrated MOTs, it is necessary to place the chips inside the vacuum chamber.

In this work, we demonstrate a compact MOT with both the grating chip and planar coil chip placed inside the vacuum chamber. The grating chip forms a tetrahedral MOT configuration, while the planar coil chip replaces conventional anti-Helmholtz coils.[17,29,30] By installing the grating chip and coil chip inside a compact vacuum chamber, we maintained a high vacuum of about $3 \times 10^{-8}\,\mathrm{mbar}$ under continuous operation. With a total chamber volume of about $20 \times 20 \times 20\,\mathrm{cm}^3$, we successfully trapped 3×10^5 cold rubidium atoms at a temperature of about $100\,\mu\mathrm{K}$. Our work paves the way for on-chip integration of atom cooling and trapping, and is promising for building hybrid quantum systems.

2. Compact MOT System. Figure 1(a) illustrates the principle of the planar-integrated MOT system,[29] which combines two key components: a grating chip and a planar coil chip. The grating chip plays a crucial role in creating the optical field necessary for atom trapping,

†These authors contributed equally to this work.
*Corresponding author. Email: clzou321@ustc.edu.cn; gyxiang@ustc.edu.cn
© 2025 Chinese Physical Society and IOP Publishing Ltd. All rights, including for text and data mining, AI training, and similar technologies, are reserved.

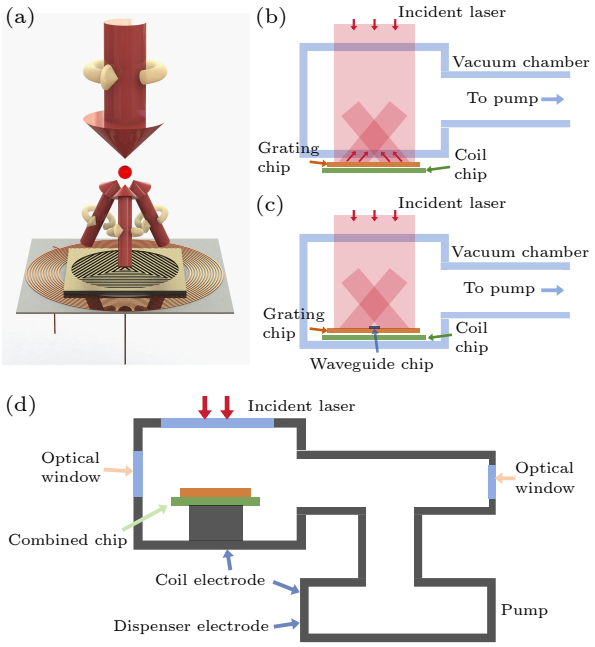

Fig. 1. (a) Planar-integrated MOT. Three linear gratings diffract the left-handed incident beam into three right-handed diffracted beams, which coincide above the chip. The working point of the planar coil chip is adjusted to the overlapping region. (b) Planar-integrated MOT with chips outside a glass vacuum cell. (c) Planar-integrated MOT with chips installed inside a glass vacuum cell. This setup allows further integration with optical waveguide chips, which could enable coupling between photons and atoms through near-field optical elements. (d) Schematic of the compact atomic system with all chips placed inside the vacuum chamber.

as demonstrated in Ref. [17]. It diffracts a single left-handed circularly polarized incident laser beam into three right-handed circularly polarized diffracted beams. These beams overlap above the chip, and the radiation pressure due to the four beams can be balanced at a certain height above the center of the chip. The planar coil chip, on the other hand, generates a quadrupole magnetic field with its zero point coinciding with the overlap region of the diffracted beams.[29] When the points of balanced force and the zero magnetic field are aligned, the combination of the optical field and the magnetic field creates a trapping potential that confines and cools the atoms, forming a MOT.

In previous works,[29] as illustrated in Fig. 1(b), the grating chip and the planar coil chip were placed outside a glass vacuum cell. While this configuration allows for easier alignment and adjustment of the chips using translation stages, it imposes limitations on the system's flexibility and potential applications. The trapped atom cloud is confined to a small distance of only about 2 mm from the cell due to the thick glass walls. Furthermore, the presence of the glass prevents the cold atomic ensemble from getting any closer to the chip, hindering the integration of additional chip elements that could enhance the functionality of the system.

To overcome these limitations and enable the integration of the MOT with other chip elements, we propose a novel design that places the grating chip and the planar coil chip inside the vacuum, as depicted in Fig. 1(c). This compact configuration offers several advantages, such as the potential for a larger space between the atom cloud and the barriers around it, which opens up new possibilities for atom manipulation and sensing applications. For instance, we can place another photonic integrated chip with a transparent substrate on top of the grating chip, enabling near-field trapping and coupling of atoms by the optical fields in the waveguide. It is also possible to place a metasurface on the grating chip, allowing for functional trapping and collection of single atoms.[46,47]

However, realizing this compact system also presents several challenges that need to be addressed. Firstly, the alignment between the grating chip and the coil chip becomes critical, as it is no longer easily tunable once the chips are placed inside the vacuum. The limited space within the chamber prevents precise and stable alignment. Secondly, the mechanical stability of the system must be ensured, including the placement of the chip holder and the wiring necessary to supply current to the chips. Vibrations or mechanical instabilities can adversely affect the performance of the MOT. Lastly, the thermal management of the system is important as the coil chip generates considerable heat during operation. In vacuum, heat dissipation is significantly reduced, which can lead to temperature gradients and thermal instabilities. Addressing these challenges requires careful design considerations, such as the use of low-outgassing materials, robust mounting mechanisms, and efficient heat dissipation techniques.

Therefore, instead of using glass cells, we propose using a vacuum chamber to address these challenges, as schematically shown in Fig. 1(d). First, we use a low-outgassing vacuum adhesive to bond the grating chip and the coil chip together. The grating chip is the same as the one used in our previous work,[29] with a grating period of 1.10 μm and a duty cycle of 0.454. To align the working point of the two chips, we initially adjust the incident light field to align with the center of the grating chip, ensuring that the intensities of the three upward-diffracted light spots are approximately equal. This indicates that the center of the light field coincides with the grating chip. Then, we use a three-dimensional displacement stage to adjust the position of the magnetic field chip so that the fluorescence of the cold atomic cloud captured by the charge-coupled device is maximized. With all chips outside the glass cell, we achieve a trapping of 3.4×10^5 cold rubidium (^{87}Rb) atoms after sub-Doppler cooling.[48] As the vacuum adhesive has a certain curing time, we can quickly adjust the position and optimize the MOT performance with the two chips outside the vacuum chamber during this period. When the vacuum adhesive is fully cured, we test the MOT performance again to make sure that the relative position between chips remains unchanged.

Instead of using a specially designed holder shown in Ref. [22], we use the same vacuum adhesive to bond the

combined chip directly to the vacuum flange protruding from the center, ensuring a stable connection. To maintain the flatness of the combined chip, we cannot directly route the wires to connect the electrode pads below the chip, as shown in Fig. 1(b). One potential approach is routing electrode pads from the center of the magnetic field to the edge of the chip via wires on printed circuit boards (PCBs). However, this approach disrupts the quadrupole magnetic field due to the lateral passage of the wires through the entire magnetic field chip. Therefore, we use conductive silver adhesive to coat one of the electrode pads to enable it to conduct directly with the flange, and the rest of the chip is bonded with low-outgassing vacuum adhesive. The remaining pads are led out from the vacuum through the wires and vacuum electrodes. As a result, the flat bonding of the combined chip is realized.

Figure 2(a) shows the photographs of the assembled vacuum system, which consists of the combined chip, a multi-window vacuum chamber, a rubidium dispenser, an ion pump, and the electrode flange of the coil chip. The vacuum chamber is made of non-magnetic stainless steel and has seven optical windows, one large window and six smaller ones. The larger window at the top is designed to allow the incident light field to illuminate the grating chip, while the six smaller windows on the sides can be used for the probe or control light fields. The entire system is mounted on a $30 \times 30\,\mathrm{cm}^2$ breadboard, with the whole chamber occupying a volume of around $20 \times 20 \times 20\,\mathrm{cm}^3$. The optical setups required for the preparation and detection of the cold atoms have been set up on this breadboard, meaning that the system possesses a certain degree of mobility. However, the lasers have not been integrated into this breadboard and need to be connected through fiber optics to the light paths for preparation and detection. From the side view of the system through a small window, as shown in Fig. 2(b), it can be seen that the grating chip, coil chip, and flange at the bottom of the vacuum chamber are flat and tightly bonded together. The grating chip used in our experiment features a gold coating, which was initially selected for its favorable optical properties. However, gold coatings can be susceptible to degradation over extended periods of operation due to interactions with alkali atoms. To mitigate this issue, aluminum provides a potential coating material with similar optical properties but with better resistance to alkali contamination.

3. Results. Before testing the cold atom trapping capability of our compact MOT system, we must consider the outgassing of all components in the vacuum chamber and the heat dissipation of the coil chip. We placed the bonded flange assembly in a separate vacuum system and conducted tests on various wire materials and conductive adhesives. Our experimental results demonstrate that using enameled wires, conductive silver adhesive and PCBs initially resulted in significant outgassing, causing the vacuum pressure to decrease more slowly. The vacuum chamber was evacuated using a turbo pump for a period of one week, resulting in a final stable pressure of 4×10^{-9} mbar, as determined by the ion pump's discharge current. During the operation of the magnetic field chip at a current of 2.5 A, the vacuum level remained stable at 3×10^{-8} mbar, indicating an acceptable level of outgassing from the chip materials.

Compared to direct placement outside the vacuum chamber, the coil chip can only dissipate heat via the connected metal flange, potentially leading to higher temperatures within the chamber. We also examined the heat dissipation of the coil chips when placed inside the vacuum. By measuring the voltage of the coil chip under different working currents after reaching thermal equilibrium, the temperature of the coil chip can be calculated from the temperature-resistance relationship of the coil material. Figure 3 shows the thermal equilibrium voltage of the coil chip under different currents. As the current increases, the stable voltage also rises, indicating an increase in the coil's resistance and suggesting a corresponding rise in temperature. When the current $I = 2.9$ A, the temperature is estimated to be about 80 °C, which is still within the normal operating temperature range of the coil chip.

When the coil chip operates continuously at a current $I = 2.5$ A, the entire system achieves a stable vacuum pressure of 3×10^{-8} mbar, with the chip temperature being approximately 65 °C. The power density at the center of the incident light field is about $20\,\mathrm{mW/cm}^2$.

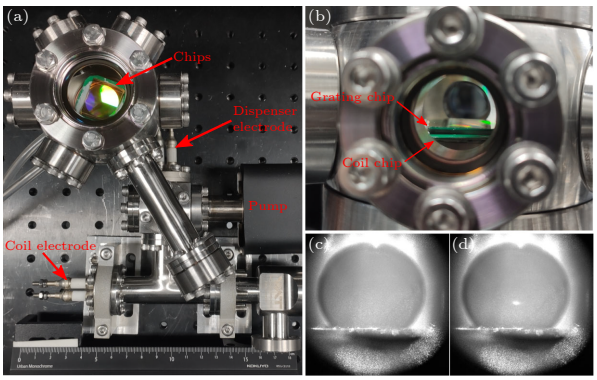

Fig. 2. (a) Photograph of the minimized atomic system. The vacuum chamber and optical setup can be placed on a $30 \times 30\,\mathrm{cm}^2$ breadboard. (b) Side view of the vacuum chamber. The combined chip is bonded to a flange at the bottom of the vacuum chamber. (c) and (d) Fluorescence images from the background (c) and trapped atoms (d), respectively, captured with a 5 ms exposure time.

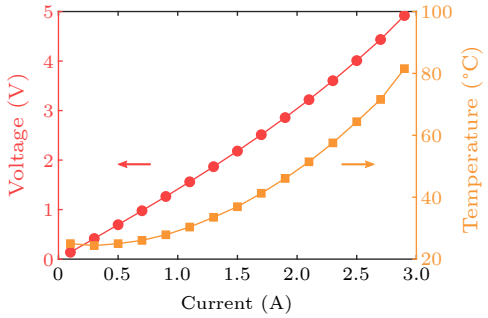

Fig. 3. Thermal equilibrium voltage and temperature of the coil chip under different currents.

We successfully trap cold ^{87}Rb atoms under these conditions. Figures 2(c) and 2(d) show the fluorescence from trapped atoms by comparing the images with and without turning on the coil chip current. The intense background light arises from scattered light from the grating chip and vacuum chamber, which can be eliminated through timing control of the incident light field and the detection light field.

We also apply polarization gradient cooling (PGC)[48] to the trapped cold atoms, with the cooling laser frequency detuning jumped by 40 MHz for a duration of 0.5 ms. Before the PGC stage, the temperature of the cold atoms in the MOT was measured to be approximately 300 μK, with an atom number of 4.7×10^5, meaning that the trap volume of our system is approximately 0.02 cm^3.[17] This relatively high initial temperature can be attributed to the limited trapping volume of our current MOT configuration. After that, we estimate that up to 3×10^5 atoms are trapped in the MOT by absorption imaging. The number of atoms trapped in the grating MOT depends on the overlap volume of the diffraction beams, laser intensity and detuning, as well as the coil current. These results indicate that the alignment, vacuum, and stability of the system are as good as placing the chips outside the vacuum. The temperature of trapped atoms is also measured with absorption imaging, by extracting the temperature from the free expansion of the atom cloud, under the assumption of a Maxwell–Boltzmann velocity distribution of the atoms.

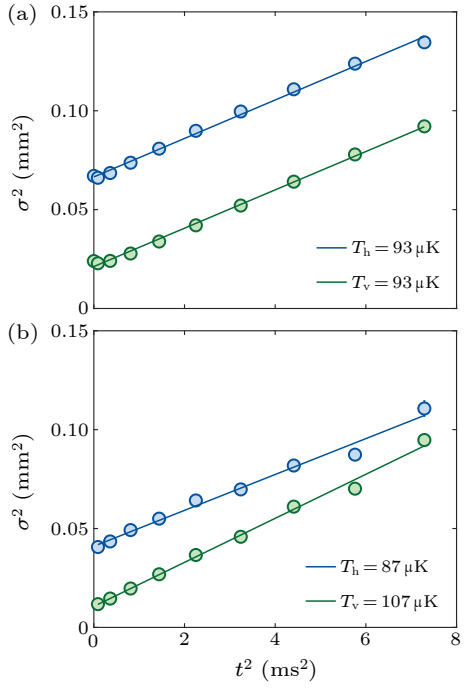

Fig. 4. The experimental and fitting results of the atom cloud sizes as functions of free expansion time. The blue and green points represent directions parallel to the chip surface and perpendicular to the chip surface, respectively. (a) All chips are placed outside the glass cell. The extracted atom temperature is about 93 μK for both horizontal and vertical directions. (b) With all chips inside the vacuum chamber, the temperatures in the two directions are 87 μK and 107 μK, respectively.

Figures 4(a) and 4(b) show the experimental and fitting results of the atom cloud sizes against free expansion time for the experimental setups with chips placed outside and inside the vacuum, respectively. Compared to the case where the chips are placed outside the vacuum chamber, which yields a measured temperature of about 93 μK, our compact MOT design exhibits similar temperatures (87 μK and 107 μK along the horizontal and vertical directions, respectively). The observed temperature difference along the vertical and horizontal directions can be primarily attributed to the asymmetric configuration of the light field. To further decrease the temperature of the cold atoms in the compact MOT, several improvements can be explored, including reshaping the incident light field and the coil chip design to increase the trapping volume,[18,49] implementing a double-MOT system,[31] and optimizing the sub-Doppler PGC cooling techniques.[19]

4. Conclusion. In summary, we have demonstrated the successful integration of a grating chip and a planar coil chip inside a compact vacuum chamber to realize a miniaturized magneto-optical trap system. We successfully trap 3×10^5 cold rubidium atoms at a temperature of about 100 μK in this minimized system, with a volume of the vacuum chamber of about $20\times20\times20$ cm^3 and a vacuum pressure of about 3×10^{-8} mbar. The system, which provides high mechanical strength and mobility, opens up new possibilities for the development of portable and versatile cold atom applications, including atomic clocks, atom interferometers, and precision measurements of electric and magnetic fields. The chip-based compact MOT system is worth further study and exploration and can potentially be improved in terms of long-term stability and integration with other photonic chip elements.

Acknowledgments. This work was supported by the National Key R&D Program (Grant Nos. 2021YFA1402004 and 2021YFF0603701), the National Natural Science Foundation of China (Grant Nos. 12134014, U21A20433, U21A6006, and 92265108), the Fundamental Research Funds for the Central Universities, and the University of Science and Technology of China (USTC) Research Funds of the Double First-Class Initiative. The numerical calculations in this paper have been done on the supercomputing system in the Supercomputing Center of the USTC. This work was partially carried out at the USTC Center for Micro and Nanoscale Research and Fabrication.

References

[1] Cronin A D, Schmiedmayer J, and Pritchard D E 2009 *Rev. Mod. Phys.* **81** 1051

[2] Ludlow A D, Boyd M M, Ye J, Peik E, and Schmidt P O 2015 *Rev. Mod. Phys.* **87** 637

[3] Weidner C and Anderson D Z 2018 *Phys. Rev. Lett.* **120** 263201

[4] Wu X, Pagel Z, Malek B S, Nguyen T H, Zi F, Scheirer D S, and Müller H 2019 *Sci. Adv* **5** eaax0800

[5] Asenbaum P, Overstreet C, Kim M, Curti J, and Kasevich M A 2020 *Phys. Rev. Lett.* **125** 191101

[6] Dudin Y, Radnaev A, Zhao R, Blumoff J, Kennedy T, and Kuzmich A 2010 *Phys. Rev. Lett.* **105** 260502

[7] Radnaev A, Dudin Y, Zhao R, Jen H, Jenkins S, Kuzmich A, and Kennedy T 2010 *Nat. Phys.* **6** 894

[8] Saffman M, Walker T G, and Mølmer K 2010 *Rev. Mod. Phys.* **82** 2313

[9] Bao X H, Reingruber A, Dietrich P, Rui J, Dück A, Strassel T, Li L, Liu N L, Zhao B, and Pan J W 2012 *Nat. Phys.* **8** 517

[10] Ding D S, Zhang W, Zhou Z Y, Shi S, Xiang G Y, Wang X S, Jiang Y K, Shi B S, and Guo G C 2015 *Phys. Rev. Lett.* **114** 050502

[11] Saffman M 2016 *J. Phys. B: At. Mol. Opt. Phys.* **49** 202001

[12] Bluvstein D, Levine H, Semeghini G, Wang T T, Ebadi S, Kalinowski M, Keesling A, Maskara N, Pichler H, Greiner M, Vuletić V, and Lukin M D 2022 *Nature* **604** 451

[13] Graham T, Song Y, Scott J, Poole C, Phuttitarn L, Jooya K, Eichler P, Jiang X, Marra A, Grinkemeyer B *et al.* 2022 *Nature* **604** 457

[14] Bluvstein D, Evered S J, Geim A A, Li S H, Zhou H, Manovitz T, Ebadi S, Cain M, Kalinowski M, Hangleiter D *et al.* 2024 *Nature* **626** 58

[15] Raab E L, Prentiss M, Cable A, Chu S, and Pritchard D E 1987 *Phys. Rev. Lett.* **59** 2631

[16] Vangeleyn M, Griffin P F, Riis E, and Arnold A S 2010 *Opt. Lett.* **35** 3453

[17] Nshii C, Vangeleyn M, Cotter J P, Griffin P F, Hinds E, Ironside C N, See P, Sinclair A, Riis E, and Arnold A S 2013 *Nat. Nanotechnol* **8** 321

[18] McGilligan J P, Griffin P F, Riis E, and Arnold A S 2016 *J. Opt. Soc. Am. B* **33** 1271

[19] McGilligan J P, Griffin P F, Elvin R, Ingleby S J, Riis E, and Arnold A S 2017 *Sci. Rep.* **7** 384

[20] McGilligan J P, Moore K R, Dellis A, Martinez G D, De Clercq E, Griffin P F, Arnold A S, Riis E, Boudot R, and Kitching J 2020 *Appl. Phys. Lett* **117** 054001

[21] Duan J, Liu X, Zhou Y, Xu X B, Chen L, Zou C L, Zhu Z, Yu Z, Ru N, and Qu J 2022 *Opt. Commun.* **513** 128087

[22] Lee J, Ding R, Christensen J, Rosenthal R R, Ison A, Gillund D P, Bossert D, Fuerschbach K H, Kindel W, Finnegan P S *et al.* 2022 *Nat. Commun.* **13** 5131

[23] Isichenko A, Chauhan N, Bose D, Wang J, Kunz P D, and Blumenthal D J 2023 *Nat. Commun.* **14** 3080

[24] Bregazzi A, Griffin P F, Arnold A S, Burt D P, Martinez G, Boudot R, Kitching J, Riis E, and McGilligan J P 2021 *Appl. Phys. Lett.* **119** 184002

[25] Dyer S, Gallacher K, Hawley U, Bregazzi A, Griffin P, Arnold A, Paul D, Riis E, and McGilligan J 2023 *Phys. Rev. Appl.* **19** 044015

[26] McGehee W R, Zhu W, Barker D S, Westly D, Yulaev A, Klimov N, Agrawal A, Eckel S, Aksyuk V, and McClelland J J 2021 *New J. Phys* **23** 013021

[27] Burrow O S, Osborn P F, Boughton E, Mirando F, Burt D P, Griffin P F, Arnold A S, and Riis E 2021 *Appl. Phys. Lett.* **119** 124002

[28] Blumenthal D J, Isichenko A, and Chauhan N 2024 *Optica Quantum* **2** 444

[29] Chen L, Huang C J, Xu X B, Zhang Y C, Ma D Q, Lu Z T, Wang Z B, Chen G J, Zhang J Z, Tang H X *et al.* 2022 *Phys. Rev. Appl.* **17** 034031

[30] Yu Z, Zhu Y, Yao M, Qi F, Chen L, Zou C L, Duan J, and Liu X 2024 *Opt. Express* **32** 8919

[31] Heine H, Arnold A S, Gonidec M S L, Griffin P F, Riis E, Herr W, and Rasel E M 2025 *New J. Phys.* **27** 033019

[32] Huang C J, Liu H C, Chen L, Li C F, Guo G C, Zou C L, and Xiang G Y 2025 *Chin. Phys. Lett.* **42** 034203

[33] Huang C J, Wang L X, Chen L, Li C F, Guo G C, Zou C L, and Xiang G Y 2025 *Chin. Phys. B* (accepted for publication)

[34] Le Kien F, Gupta S D, Balykin V, and Hakuta K 2005 *Phys. Rev. A* **72** 032509

[35] Vetsch E, Reitz D, Sagué G, Schmidt R, Dawkins S, and Rauschenbeutel A 2010 *Phys. Rev. Lett.* **104** 203603

[36] Dawkins S, Mitsch R, Reitz D, Vetsch E, and Rauschenbeutel A 2011 *Phys. Rev. Lett.* **107** 243601

[37] Thompson J D, Tiecke T, de Leon N P, Feist J, Akimov A, Gullans M, Zibrov A S, Vuletić V, and Lukin M D 2013 *Science* **340** 1202

[38] Kato S and Aoki T 2015 *Phys. Rev. Lett.* **115** 093603

[39] González-Tudela A, Hung C L, Chang D E, Cirac J I, and Kimble H 2015 *Nat. Photonics* **9** 320

[40] Sayrin C, Clausen C, Albrecht B, Schneeweiss P, and Rauschenbeutel A 2015 *Optica* **2** 353

[41] Solano P, Barberis-Blostein P, Fatemi F K, Orozco L A, and Rolston S L 2017 *Nat. Commun.* **8** 1

[42] Béguin J B, Müller J H, Appel J, and Polzik E S 2018 *Phys. Rev. X* **8** 031010

[43] Chang D, Douglas J, González-Tudela A, Hung C L, and Kimble H 2018 *Rev. Mod. Phys.* **90** 031002

[44] Corzo N V, Raskop J, Chandra A, Sheremet A S, Gouraud B, and Laurat J 2019 *Nature* **566** 359

[45] Yang P, Xia X, He H, Li S, Han X, Zhang P, Li G, Zhang P, Xu J, Yang Y *et al.* 2019 *Phys. Rev. Lett.* **123** 233604

[46] Kim M E, Chang T H, Fields B M, Chen C A, and Hung L 2019 *Nat. Commun.* **10** 1647

[47] Hsu T W, Zhu W, Thiele T, Brown M O, Papp S B, Agrawal A, and Regal C A 2022 *PRX Quantum* **3** 030316

[48] Dalibard J and Cohen-Tannoudji C 1989 *JOSA B* **6** 2023

[49] McGilligan J P, Griffin P F, Riis E, and Arnold A S 2015 *Opt. Express* **23** 8948